11th ANKARA INTERNATIONAL AEROSPACE CONFERENCE **AIAC-2021-162**
8-10 September 2021 - METU, Ankara TURKEY

LOW-ENERGY AND LOW-THRUST LUNAR TRAJECTORY DESIGN USING PARTICLE SWARM OPTIMIZATION

Mehmet Fatih Ertürk*
Istanbul Technical University, Istanbul

Şahin Ulaş Köprücü†
Middle East Technical University, Ankara

Nevsan Şengil‡
Tahsin Çağrı Şişman§
Mecit Yaman¶
University of Turkish Aeronautical Association, Ankara

ABSTRACT

We designed a low-energy, low-thrust Lunar trajectory by using particle swarm optimization (PSO). We optimized the transfer trajectory with the cost function of minimum fuel mass. First we discussed the sensitivity of the orbit propagation to the initial condition due to the chaotic nature of the three-body problem. Then, we considered a low-thrust Lunar orbit insertion strategy and applied PSO to minimize total fuel mass required for the transfer. Finally, we found the fuel mass considerably smaller than our previous work.

INTRODUCTION

CubeSats are a class of nanosatellites having a standard for design to reduce the cost and development time for space missions. Since they provide cost-effective solutions, the number of CubeSat missions continuously increase with wide range of applications. Most of the CubeSat missions are designed for low Earth orbit (LEO), but there are also some deep space missions. For example, Mars Cube One (MarCO) launched at 2018 was the first mission to prove the capability of CubeSats for the deep space missions [NASA, 2020]. The two MarCO CubeSats of 6U size were part of the NASA's InSight mission to act as communication relay for InSight during the "7 minutes of terror" in the Martian atmosphere as InSight landed on Mars. Furthermore, Artemis I which is going to be the first test flight of the new crewed missions era for the Moon will also deploy 13 CubeSats in a trans-lunar trajectory. These CubeSats will carry out deep space scientific research and perform technology demonstrations [NASA, 2019]. Artemis I with a planned launch on 2021 will have an impact for the future Moon and Mars missions including the CubeSat based ones.

In the National Space Program of Turkey, it is aimed to have hard landing on the Moon at 2023 and soft landing at 2028 [TSA, 2021]. For the soft-landing mission, it is planned to use ingenuously

*Student, Aeronautics and Astronautics Engineering, Email: erturkm19@itu.edu.tr
†Student, Physics, Email: ulas.koprucu@metu.edu.tr
‡Prof., Astronautical Engineering, Email: nsengil@thk.edu.tr
§Prof., Astronautical Engineering, Email: tcsisman@thk.edu.tr
¶Assoc. Prof., Aeronautical Engineering, Email: myaman@thk.edu.tr

developed rocket and propulsion system capabilities from launch to trans-lunar injection and lunar landing. In this respect, the Hall thruster HALE [TUBITAK-UZAY, 2021] developed by TUBITAK Space Technologies Research Institute (TUBITAK-UZAY) may also serve as a propulsion system for the future Moon missions of Turkey just like the electric propulsion based SMART-1 mission of European Space Agency (ESA).

In this paper, we would like to support this vision of Moon missions with the CubeSat based mission alternatives. The mission proposals in this paper are mainly inline with the CubeSat missions of the Artemis I. We developed low-energy Moon transfer trajectory alternatives based on mainly electric propulsion systems. In this respect, for example, the Lunar IceCube which is one of the 13 CubeSats of Artemis I also has a similar transfer trajectory design again with the use of an electric propulsion system [Folta et. al., 2016].

For deep space missions, the electric propulsion systems are preferred for their high specific impulse (Isp) values resulting less amount of fuel. Thus, compared to chemical propulsion systems, these propulsion systems have smaller launch mass. With the advent of electric propulsion systems for the CubeSat platforms, it becomes feasible to plan CubeSat missions beyond LEO by taking the advantage of reduced fuel mass of the electric propulsion systems. On the other hand, the thrust provided by these systems are small compared to the chemical propulsion systems. Therefore, in this study, we preferred the electric propulsion as the main propulsion system to take the advantage of reduced fuel mass, and to deal with the downside of small thrust, we focused on the low-energy transfer trajectories.

In planning the Earth to Moon transfer trajectory, one may have three options in general. The first option is the Hohmann transfer orbit which is the most frequently used transfer method. The required velocity change is calculated with the basic two-body calculations. For the Moon mission, there are two different two-body problems which are Earth-spacecraft and Moon-spacecraft systems. The Hohmann transfer method requires impulsive maneuvers; so that, a chemical propulsion is more suitable choice to inject the spacecraft to the transfer orbit. The second option is the low-energy transfer trajectory [Belbruno and Miller, 1993] which requires less fuel with respect to the Hohmann transfer orbit. In this method, the trajectory is designed in the context of two separate restricted three-body problem which are the Earth-Sun-spacecraft and Earth-Moon-spacecraft systems [Koon et. al., 2016]. The dynamical structure of these systems enable to reach lunar orbit with less fuel compared to the Hohmann transfer orbit. The low-energy trajectories are suitable for the use of low-thrust maneuvers in addition to impulsive maneuver alternatives. Thus, it is possible to use the electric propulsion systems for this transfer trajectory option. The last option is the spiral transfer in which only the low-thrust propulsion system is employed to have a spiralling out trajectory starting from possibly LEO till to the Moon.

Now, let us consider the three transfer trajectory design options for a lunar CubeSat mission. If one applies the Hohmann transfer method in a lunar CubeSat mission, its fuel requirements would be large due to impulsive maneuver needs which in turn scales up the spacecraft from a nanosatellite to microsatellite. Due to reduced fuel mass requirements of the electric propulsion systems, the other two options of lunar transfer trajectory; namely, the low-energy transfer trajectory and the spiral trajectory, which are suitable for the use of the electric propulsion systems seem more feasible for a lunar CubeSat mission. For the spiral trajectory, there would be a need for a larger Delta-V maneuver at the lunar capture while for the low-energy transfer trajectory, there is the possibility to have a ballistic lunar capture. Thus, we focus on the low-energy trajectory design in this study.

In this paper, first we studied how precise the patch point of the low-energy transfer trajectory should be defined. Due to the chaotic nature of the three-body problem, the trajectory design is highly sensitive to the state vector at the patch point. After fixing the patch point properly, we carry out a particle swarm optimization (PSO) based trajectory design with the cost function of minimizing the total fuel mass by varying the velocity vectors at the patch point and the duration of propagation. We tried to minimize overall fuel mass arises from the Earth departure, patch point and Moon arrival maneuvers. We considered a low-thrust Lunar orbit insertion (LOI) strategy as

distinct from our previous work which was done with an impulsive maneuver. The calculation of the injection maneuvers require a special care. Because the velocities at the spiral trajectories are defined in the Earth-centered inertial frame for the departure part and Moon-centered inertial frame for the arrival part while the velocities at the low-energy departure and low-energy arrival trajectories are defined in the rotating frame of Sun-Earth system. Thus, to determine the required Δv properly, it is necessary to make coordinate transformation. With considering this, we applied PSO to obtain a trajectory which minimizes the total fuel mass.

METHOD

In this part, firstly our previous work is briefly summarized. Then, the sensitivity to the initial conditions and the low-thrust LOI strategy are discussed, respectively. Lastly, the required frame transformation is explained.

In the previous work, we studied the preliminary orbit design for a Lunar CubeSat mission with an electric propulsion system by focusing on the departure part. The idea was attaining to a low-energy transfer trajectory from LEO by using an electric propulsion system. Since the main interest was on the Earth departure part, the initial conditions given in [Onozaki et. al., 2017] was used for the low-energy transfer trajectory design. In the low-thrust Earth departure strategy, we considered that CubeSat applies continuous low-thrust along the velocity vector and make spiral out transfer until a point where the injection to the low-energy transfer trajectory occurs. In order to find the injection point, PSO was used such that the velocity vectors belonging to patch point and the duration of propagation were considered as design variables to find an injection point which minimizes the total fuel. The total fuel includes necessary fuels for low-thrust spiral out transfer, injection maneuver, patch point maneuver and lastly LOI maneuver. Trajectory obtained from the PSO was presented with the total fuel and transfer time in the previous work. In addition to the low-energy transfer trajectory, spiral transfer to the Moon was also investigated and compared. The detailed discussions can be found in our previous work [Ertürk et. al., 2020].

The sensitivity analysis to the initial condition is an important issue in this study due to the chaotic nature of the three-body problem. In this respect, firstly, the initial conditions given in [Onozaki et. al., 2017] are examined such that the initial conditions belonging to patch points are propagated backward and forward up to the initial conditions belonging to Earth departure and Moon arrival points, respectively. Orbit is propagated through the equations of motion of bicircular restricted four-body problem [Onozaki et. al., 2017]. Solver is chosen as MATLAB ode45 built-in function with the absolute and relative tolerance of 10^{-6} and with the maximum step size of 10^{-4}. Also note that the normalized units are used, namely one unit distance is equal to a_s which is the distance between Sun and Earth-Moon barycenter, one unit time is equal to $1/w_s$ where w_s is the angular velocity of the Sun and Earth-Moon barycenter. The details can be found in [Onozaki et. al., 2017] and [Ertürk et. al., 2020].

Table 1: Initial conditions given in [Onozaki et. al., 2017]

	$\bar{x}$	$\bar{y}$	$\dot{\bar{x}}$	$\dot{\bar{y}}$	$\overline{\theta}_M$ (rad)
Patch Point (Earth Part)	1.00507	0	−0.0113680	0.0175449	4.96074
Earth Departure Point	0.999922	0	0	−0.368963	0
Patch Point (Moon Part)	1.00507	0	−0.0121205	0.0184927	4.96074
Moon Arrival Point	0.997900	0.00140873	0.0249961	0.0372041	2.55000

From Table 2, it is clearly seen that one could not obtain the Earth departure and Moon arrival points from the backward and forward propagation of the corresponding patch point with the given precision. To satisfy those points, we considered to increase precision of only $\bar{x}$ component of the patch point. Since position is same for both Earth and Moon parts of the patch point, we are able to check departure and arrival points by improving only a single component. PSO is used to determine

Table 2: Earth departure and Moon arrival points which are propagated from the corresponding patch point

	$\bar{x}$	$\bar{y}$	$\dot{\bar{x}}$	$\dot{\bar{y}}$	$\overline{\theta}_M$ (rad)
Patch Point (Earth Part)	1.00507	0	−0.0113680	0.0175449	4.96074
Earth Departure Point	1.001157	0.000455	−0.061444	−0.010836	0
Patch Point (Moon Part)	1.00507	0	−0.0121205	0.0184927	4.96074
Moon Arrival Point	0.997889	0.00139872	0.0401007	0.0033477	2.55000

precise $\bar{x}_P$ such that $\bar{x}_P$ is changed to minimize sum of the differences between the propagated states and the states given in [Onozaki et. al., 2017].

Table 3: Earth departure and Moon arrival points which are propagated from the corresponding precise patch point

	$\bar{x}$	$\bar{y}$	$\dot{\bar{x}}$	$\dot{\bar{y}}$	$\overline{\theta}_M$ (rad)
Patch Point (Earth Part)	1.0050749564919628	0	−0.0113680	0.0175449	4.96074
Earth Departure Point	0.999922	$\approx 4 \times 10^{-11}$	$\approx 3 \times 10^{-10}$	−0.368963	0
Patch Point (Moon Part)	1.0050749564919628	0	−0.0121205	0.0184927	4.96074
Moon Arrival Point	0.997900	0.00140869	0.0251343	0.0371034	2.55000

From the PSO, $\bar{x}_P$ is found as 1.0050749564919628. The initial conditions are given in [Onozaki et. al., 2017] with 6 significant figures for the Earth departure part. When the precise patch point belonging to Earth part is propagated backward until the departure point, this propagated state match with [Onozaki et. al., 2017] at 6 significant figures. However, the same precision could not be obtained for the arrival point.

Since the nature of the problem is chaotic, it is important to investigate sensitivity to the initial conditions. The question is that what precision is required for the patch point to satisfy the Earth departure point. In order to answer this question, $\bar{x}_P$ found from the PSO is written with different precisions and its effect on the Earth departure point is examined.

Table 4: Earth departure points obtained from the patch points with different precisions

	$\bar{x}$	$\bar{y}$	$\dot{\bar{x}}$	$\dot{\bar{y}}$	$\overline{\theta}_M$ (rad)
Patch Point (Earth Part)	1.005074956491962768	0	−0.0113680	0.0175449	4.96074
Earth Departure Point	0.999922	$\approx 4 \times 10^{-11}$	$\approx 3 \times 10^{-10}$	−0.368963	0
Patch Point (Earth Part)	1.0050749564919277	0	−0.0113680	0.0175449	4.96074
Earth Departure Point	0.999922	$\approx 4 \times 10^{-11}$	$\approx 3 \times 10^{-10}$	−0.368963	0
Patch Point (Earth Part)	1.0050749564919628	0	−0.0113680	0.0175449	4.96074
Earth Departure Point	0.999922	$\approx 4 \times 10^{-11}$	$\approx 3 \times 10^{-10}$	−0.368963	0
Patch Point (Earth Part)	1.005074956491963	0	−0.0113680	0.0175449	4.96074
Earth Departure Point	0.999922	$\approx 4 \times 10^{-11}$	$\approx 7 \times 10^{-10}$	−0.368963	0
Patch Point (Earth Part)	1.00507495649196	0	−0.0113680	0.0175449	4.96074
Earth Departure Point	0.999922	$\approx 4 \times 10^{-11}$	$\approx -1 \times 10^{-8}$	−0.368963	0

From Table 4, it is seen that the required precision is belonging to $\bar{x} = 1.0050749564919628$. Below this precision, $\dot{\bar{x}}$ component of the Earth departure point starts to change and above this precision, there is no change in the departure point.

In the low-thrust LOI, we actually applied the same strategy as we did in the Earth departure part. The arrival trajectory is propagated forward from the patch point during the given duration and the points which are inside the sphere of influence of the Moon are obtained. For all of these points, it is considered firstly that CubeSat applies an impulsive maneuver to match its arrival velocity vector with the velocity vector required to be on the inward spiral trajectory. Another words, this impulsive maneuver is required to put the CubeSat from arrival trajectory to the inward spiral trajectory.

Then, CubeSat lowers the altitude to $100\,\mathrm{km}$ by applying continuous low-thrust along opposite to the velocity vector in the inward spiral trajectory and it reaches to the $100\,\mathrm{km}$ circular Lunar orbit at the end. The similar discussion for the low-thrust Earth departure strategy and also the necessary equations to calculate fuel due to low-thrust with the thruster properties can be found in [Ertürk et. al., 2020].

In the calculation of the impulsive maneuver for injection from outward spiral trajectory to the low-energy departure trajectory and insertion from low-energy arrival trajectory to the inward spiral trajectory, frame transformation is required. The impulsive maneuver can be simply calculated from

$$\Delta v = \sqrt{v_1^2 + v_2^2 - 2v_1 v_2 \cos\gamma}. \tag{1}$$

Here, v_1 is the velocity of the CubeSat in the low-energy transfer trajectory, v_2 is the velocity of the CubeSat in the spiral trajectory, and γ is the angle between those vectors. Here, v_2 is defined in Earth-centered inertial frame for the departure part and Moon-centered inertial frame for the arrival part while v_1 is defined in the rotating frame of bicircular restricted four-body problem. In order to resolve this frame differences, the following basic frame transformation is used

$$\vec{v}_{S/C,abs} = \vec{w}_s \times \vec{r}_{S/C,rot} + \vec{v}_{S/C,rot}, \tag{2a}$$

$$\vec{v}_{Earth/Moon,abs} = \vec{w}_s \times \vec{r}_{Earth/Moon,rot} + \vec{v}_{Earth/Moon,rot}, \tag{2b}$$

$$\vec{v}_1 = \vec{v}_{S/C,abs} - \vec{v}_{Earth/Moon,abs}. \tag{2c}$$

Particle Swarm Optimization

PSO is a type of evolutionary algorithm which mimics the droves. Each member of drove or in our case swarm is named as particle (x). PSO drives the members of drove to a targeted place. In other words, PSO iterates the particles of a swarm to reach the global minimum of the cost function. This iterative process leads up until termination criteria satisfies. Limiting the maximum number of iteration is also possible. In this study, the implemented code of [Ertürk et. al., 2020] is used again. The code is a modified version of [Heris, 2015].

Algorithm 1: Particle Swarm Optimization Main Algorithm

Result: Optimized total fuel mass
initialization;
for *i=1 to number of swarm size* **do**
  Randomize the particles on the swarm;
  Calculate the cost of particle
end
Define the best particle in swarm ($\vec{P}_{Best}$) and global best particle ($\vec{G}_{Best}$);
for *j=1 to number of maximum iteration* **do**
  for *i=1 to number of swarm size* **do**
    $\vec{v}_{ij} = w\vec{v}_{ij} + c_1\vec{r}_1\left[\vec{P}_{Best} - \vec{x}_{ij}\right] + c_2\vec{r}_2\left[\vec{G}_{Best} - \vec{x}_{ij}\right]$;
    $\vec{x}_{ij} = \vec{x}_{ij} + \vec{v}_{ij}$
  end
  Update $\vec{P}_{Best}$ and $\vec{G}_{Best}$;
  Check the termination criteria, if any is satisfied terminate the iterations;
  $w = w * w_{damp}$;
end

Termination criteria of the PSO count the non-decreasing accuracy of ordered results. This count is also known as stall iteration. If the change in result is below 10^{-3}, that equals 1 gram change in total fuel mass, count starts until it reaches 0 to 7. The accuracy is defined as 10^{-3}, because lower results will be meaningless in terms of reality. Number of stall iteration is defined after trial and error.

RESULTS AND DISCUSSION

In this part, firstly our previous results in [Ertürk et. al., 2020] are represented with the precise patch point including the frame transformation. Then, the results of PSO which minimizes the overall fuel mass considering the low-thrust LOI strategy are given.

Firstly, our previous results are given with only considering the frame transformation while the precise patch point is not used.

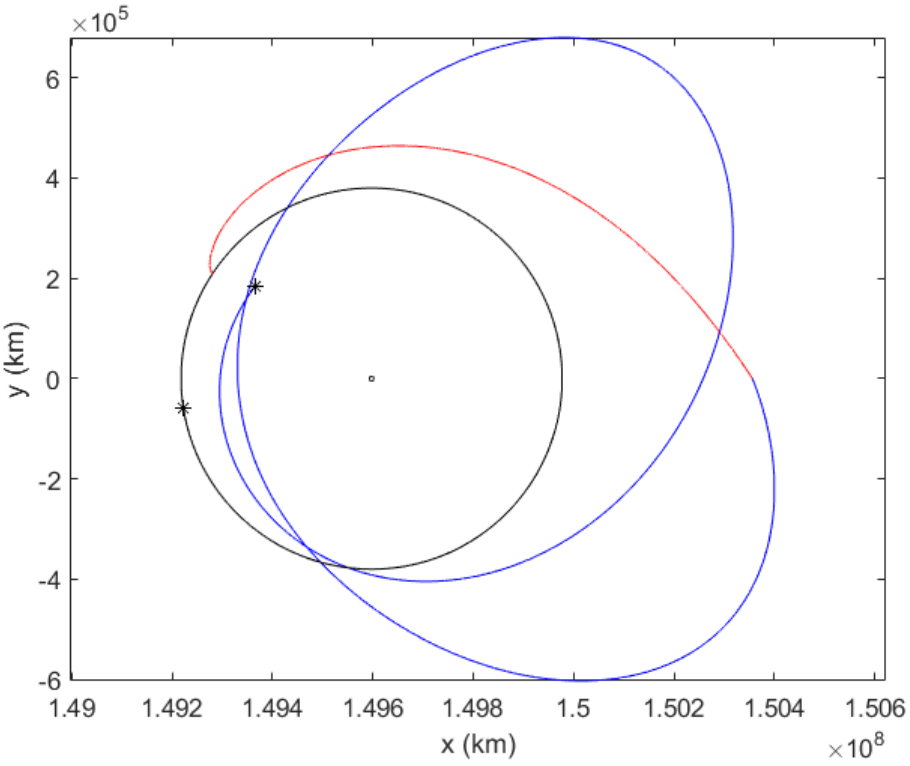

Figure 1: The transfer trajectory obtained with considering only the frame transformation

Table 5: Initial conditions at the patch point for the corresponding part of the trajectories in Figure 1

	$\bar{x}_P$	$\bar{y}_P$	$\dot{\bar{x}}_P$	$\dot{\bar{y}}_P$	$\overline{\theta}_M$ (rad)
Blue trajectory	1.00507	0	−0.0060967	0.0154186	4.96074
Red trajectory	1.00507	0	−0.0121205	0.0184927	4.96074

In Figure 1, blue and red trajectories illustrate the departure and arrival trajectories, respectively. The corresponding initial condition for each one is also given in Table 5, namely blue and red trajectories are obtained from backward and forward integration of the corresponding initial condition. The starred point on the departure trajectory represents the injection point. The CubeSat applies continuous tangential thrust until reach that point, then injection maneuver is applied to put the CubeSat in low-energy transfer trajectory. Also the starred point on the black trajectory represents the Moon's position at the time that injection maneuver occurs.

Table 6: Fuel masses and transfer time for the trajectory in Figure 1

$m_{electric,Earth}$	$m_{injection,Earth}$	m_{patch}	m_{LOI}	T
2.7 kg	0.16 kg	0.44 kg	1.2 kg	146 days

The transfer time and the required fuel masses for the maneuvers of a Cubesat with dry mass of

5 kg are given in Table 6. Here m_{LOI} and m_{patch} are the necessary fuel masses for the LOI and the patch point maneuvers, respectively. Due to the frame transformation applied in the calculation of injection maneuver, necessary fuel mass for the injection maneuver $m_{injection,Earth}$ is different from our previous result. Actually, there was no need for any injection maneuver in the previous result. But after the frame transformation, injection maneuver is found as $0.069\,\mathrm{km/s}$. Lastly, $m_{electric,Earth}$ is the fuel mass used in the spiral out transfer with electric propulsion from LEO to the injection point.

Secondly, our previous results are given with the precise patch point including the frame transformation.

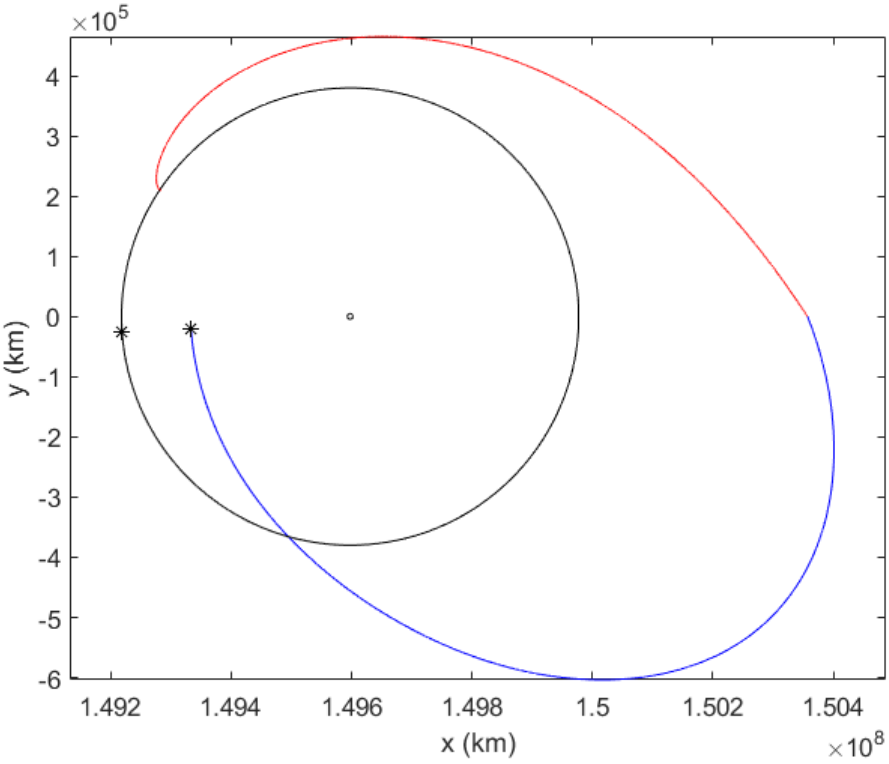

Figure 2: The transfer trajectory obtained from the precise patch point including the frame transformation

Table 7: Initial conditions at the patch point for the corresponding part of the trajectories in Figure 2

	$\bar{x}_P$	$\bar{y}_P$	$\dot{\bar{x}}_P$	$\dot{\bar{y}}_P$	$\bar{\theta}_M$ (rad)
Blue trajectory	1.0050749564919628	0	−0.0060967	0.0154186	4.96074
Red trajectory	1.0050749564919628	0	−0.0121205	0.0184927	4.96074

Table 8: Fuel masses and transfer time for the trajectory in Figure 2

$m_{electric,Earth}$	$m_{injection,Earth}$	m_{patch}	m_{LOI}	T
3.0 kg	0.87 kg	0.44 kg	1.2 kg	90 days

In Table 8, the transfer time and the required fuel masses are given for the case when the precise patch point is used with the frame transformation. The total fuel mass is about 5.5 kg which is in fact large compared to the previous result. In order to reduce overall fuel mass, we used PSO with the low-thrust Moon arrival strategy.

PSO is iterated 125 times in a way that to minimize total fuel mass by considering the low-thrust LOI strategy. The solution with minimum fuel requirement is chosen to be presented in Figure 3.

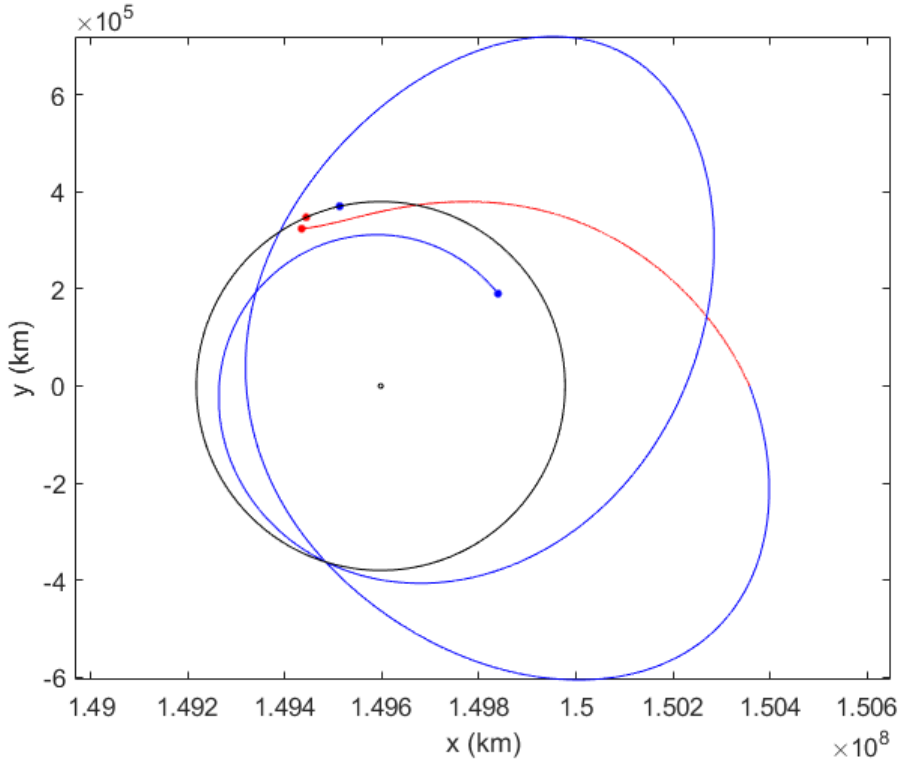

Figure 3: The optimum solution obtained from the PSO

Table 9: Initial conditions at the patch point for the corresponding part of the trajectories in Figure 3

	$\bar{x}_P$	$\bar{y}_P$	$\dot{\bar{x}}_P$	$\dot{\bar{y}}_P$	$\bar{\theta}_M$ (rad)
Blue trajectory	1.0050749564919628	0	−0.0058691491631227	0.0155046427477200	4.96074
Red trajectory	1.0050749564919628	0	−0.0064247390098674	0.0144002712742782	4.96074

In Figure 3, blue point on the departure trajectory represents the injection point from low-thrust outward spiral to the low-energy transfer trajectory, and blue point on the Moon's orbit represents the position of the Moon at the time that injection maneuver occurs. In the same manner, red point on the arrival trajectory represents the injection point from low-energy transfer trajectory to the low-thrust inward spiral.

Table 10: Fuel masses of the maneuvers and transfer time for the trajectory in Figure 3

$m_{electric,Earth}$	$m_{injection,Earth}$	m_{patch}	$m_{electric,Moon}$	$m_{injection,Moon}$	T
2.3 kg	0.047 kg	0.071 kg	0.31 kg	0.33 kg	149 days

The total fuel mass is found about 3.1 kg for a CubeSat with dry mass of 5.0 kg. This total fuel mass is considerably smaller than the previous result which is 5.5 kg. In addition, the fuel mass for each maneuver also decreased, and there is a more smooth transition at the patch point compared to the previous result. Especially, most of the reduction occurred in the Moon part thanks to the low-thrust LOI strategy.

We also looked for the minimization pattern in the 125 solutions obtained from the PSO and we presented the required fuel masses for the each maneuver in each solution in Figure 4 and Figure 5.

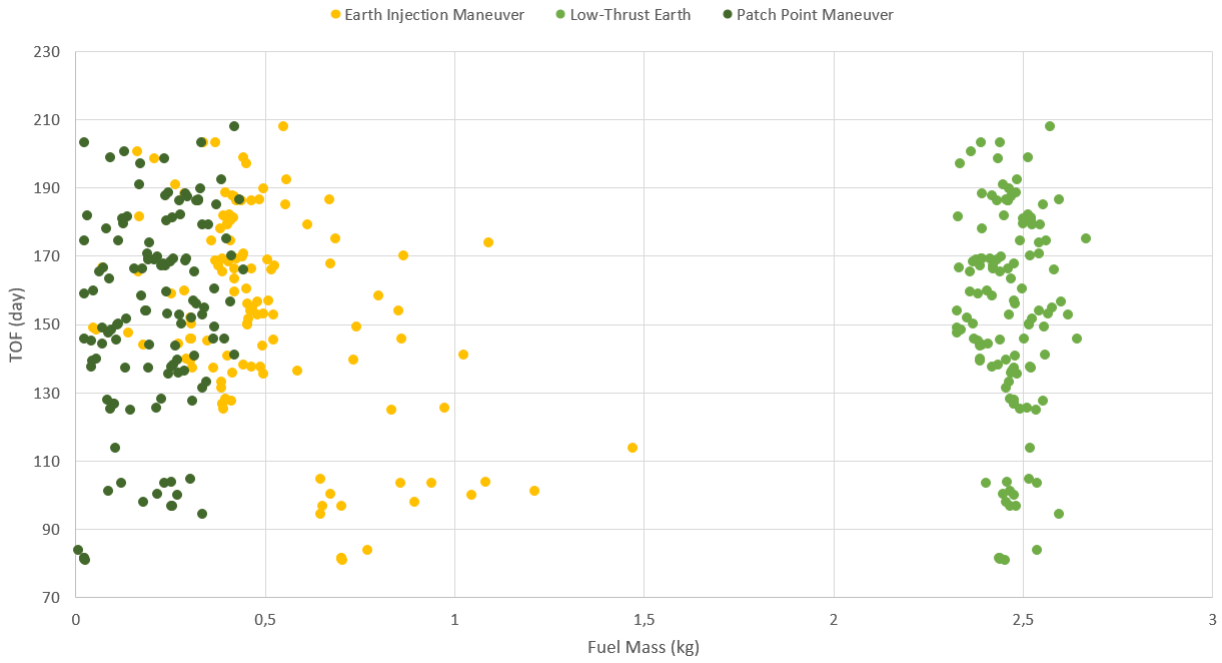

Figure 4: The required fuel masses due to Earth injection maneuver, low-thrust outward spiral maneuver and patch point maneuver obtained in each solution with the time of flight (TOF)

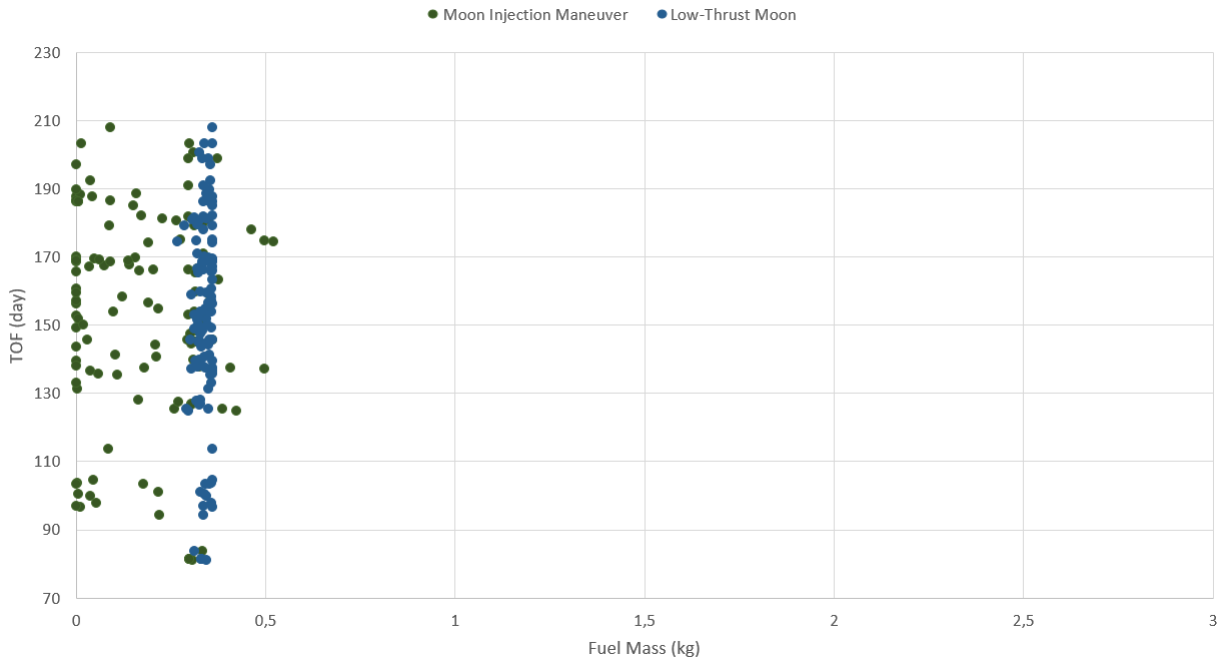

Figure 5: The required fuel masses due to Moon injection maneuver and low-thrust inward spiral maneuver obtained in each solution with the TOF

In the 125 solutions, the fuel mass changes within a narrow interval for the low-thrust outward and low-thrust inward maneuvers which means PSO could not minimize fuel masses due to those maneuvers. On the other hand, the fuel mass due to the Earth injection maneuver change within a wider range, and therefore we can conclude that minimization mainly occurs in the Earth injection maneuver.

CONCLUSIONS

In this work, we propose a Moon mission by designing a low-energy and low-thrust Earth to Moon trajectory by using PSO. We optimized the transfer trajectory with the cost function of minimum fuel mass. In doing this optimization, fixing the patch point position precisely is an important issue due to sensitivity of the orbit propagation to initial conditions. After fixing the patch point properly, we carry out the PSO by varying the velocity vectors at the patch point and the duration of the propagation. From the PSO, we found that the minimum total fuel mass is about $3.1\,\mathrm{kg}$ which is considerably smaller than the previous result ($5.5\,\mathrm{kg}$) thanks to the low-thrust LOI strategy. Also, we observed that minimization mainly occurs in the Earth injection maneuver. As a future work, implemented algorithm will be run for a micro satellite system with only electric propulsion to make the results more realistic. Additionally, changing the position of patch point will be also considered.

References

Belbruno, E. A. ve Miller, J. K. (1993) *Sun-Perturbed Earth-to-Moon Transfers with Ballistic Capture*, Journal of Guidance, Control and Dynamics, Vol. 16, No. 4.

Ertürk, M. F., Köprücü, Ş. U., Gomroki, M. M., Şengil, N., Şişman, T. Ç. and Yaman, M. (2020) *Preliminary Orbit Design for a Lunar Cubesat Mission*, National Aerospace Conference, Ankara, Turkey.

Folta, D. C., Bosanac, N., Cox, A. and Howell, K. C. (2016) *The Lunar IceCube Mission Design: Construction of Feasible Transfer Trajectories with a Constrained Departure*, 26th AAS/AIAA Space Flight Mechanics Meeting.

Heris, M. K. (2015) *Online: Particle Swarm Optimization in MATLAB*, Accessible: https://yarpiz.com/50/ypea102-particle-swarm-optimization, Access Date: 04.07.2021

Koon, W. S., Lo, M. W., Marsden, J. E. and Ross, S. D. (2001) *Low Energy Transfer to the Moon*, Celestial Mechanics and Dynamical Astronomy, Vol. 81, pp. 63-73.

NASA (2019) *Online: Artemis-I Overview*, Accessible: https://www.nasa.gov/content/artemis-i-overview, Access Date: 16.08.2020

NASA (2020) *Online: Mars Cube One (MarCO)*, Accessible: https://www.jpl.nasa.gov/cubesat/missions/marco.php, Access Date: 16.08.2020

Onozaki, K., Yoshimura, H. and Ross, S. D. (2017) *Tube dynamics and low energy Earth-Moon transfers in the 4-body system*, Advances in Space Research, Vol. 60, pp. 2117-2132.

TSA (2021) *Online: Türkiye'nin Uzay Yolculuğu Başlıyor*, Accessible: https://tua.gov.tr/tr/haberler/turkiye-nin-uzay-yolculugu-basliyor, Access Date: 28.03.2021

TUBITAK-UZAY (2021) *Online: HALE*, Accessible: https://uzay.tubitak.gov.tr/en/uydu-uzay/hale, Access Date: 30.07.2021